

INTERPRETATION OF MÖSSBAUER SPECTRA OF NONTRONITE, CELADONITE, AND GLAUCONITE

LYDIA G. DAYNYAK AND V. A. DRITS

Geological Institute of the U.S.S.R. Academy of Sciences
Moscow, U.S.S.R

Abstract—A new approach to the interpretation of Mössbauer spectra of Fe³⁺-phyllosilicates having vacant trans-octahedra is based on (1) crystal structure simulation methods that allow for the size and the shape of a Fe³⁺-octahedron as a function of the nearest surrounding cations; and (2) calculations of electric field gradients (EFG) on Fe³⁺ in terms of the ionic point-charge model. Calculations were performed by direct summation within the region of radius ≤ 50 Å. Coordinates for the anions in the coordination octahedra have been assigned to take into account the nearest cationic environment. Atomic coordinates for the rest of the summation volume are those for the average unit cell. EFG calculations for cation combinations responsible for the visible quadrupole splitting Δ_{vis} in the spectra of nontronite, “red” muscovite, and celadonite have led to good agreement between Δ_{vis} and Δ_{calc} . Computer fitting of the nontronite and celadonite spectra based on EFG calculations for the rest of the possible cation combinations suggests that the distribution of tetrahedral cations in nontronite obeys the Loewenstein rule, and in celadonite, the distribution of R³⁺ and R²⁺ over cis-octahedra is predominantly ordered, in agreement with electron diffraction and infrared spectroscopy data. The Mössbauer spectrum of one of the glauconites suggested the presence of celadonite-like and muscovite-like domains in its 2:1 layers.

Key Words—Atomic coordinates, Celadonite, Electric field gradient, Glauconite, Mössbauer spectroscopy, Nontronite.

Резюме—Описан новый подход к интерпретации мессбауэровских спектров Fe³⁺-филлосиликатов с вакантными транс-октаэдрами. Он основан на: (1) применении методов структурного моделирования, позволяющих учитывать размер и форму Fe³⁺-октаэдра в зависимости от ближайших окружающих катионов; (2) расчетах градиентов электрических полей (ГЭП) на ядре Fe³⁺ в модели ионных точечных зарядов. Расчеты выполнялись прямым суммированием в области радиусом ≤ 50 Å. Координаты анионов координирующего октаэдра задавались в соответствии с ближайшим катионным окружением. В остальной области суммирования использовались координаты атомов усредненной элементарной ячейки.

Расчеты ГЭП для комбинаций катионов, ответственных за видимое квадрупольное расщепление $\Delta_{\text{вид}}$ в спектрах нонтронита, “красного” мусковита и селадонита, привели к хорошему согласию между $\Delta_{\text{вид}}$ и $\Delta_{\text{расч}}$. Из разложения спектров нонтронита и селадонита, основанного на расчетах ГЭП для остальных возможных комбинаций, следует, что распределение тетраэдрических катионов в нонтроните подчиняется правилу Левенштейна, а в селадоните распределение катионов R³⁺ и R²⁺ по цис-октаэдрам является преимущественно упорядоченным, что согласуется с электронографическими и ИК-спектроскопическими данными.

Из анализа мессбауэровского спектра одного из глауконитов следует наличие селадонитоподобных и мусковитоподобных доменов в 2:1 слоях его структуры.

Обсуждаются методологические аспекты интерпретации мессбауэровских спектров диоктаэдрических филлосиликатов.

INTRODUCTION

To date, there has been no consistent interpretation of the Mössbauer spectra of dioctahedral layer silicates. Most workers have treated the spectra of celadonite (Malysheva *et al.*, 1976), nontronite (Goodman *et al.*, 1976; Heller-Kallai and Rozenson, 1981), glauconites (Rozenson and Heller-Kallai, 1978; McConchie *et al.*, 1979; Govaert *et al.*, 1979; Kotlicki *et al.*, 1981) as the superposition of two doublets related to Fe³⁺ ions in cis- and trans-octahedra. According to X-ray and electron diffraction data, trans-octahedral sites of the 2:1 layers of these minerals are vacant (Tsipursky *et al.*, 1978; Daynyak *et al.*, 1981a; Besson *et al.*, 1983; Tsipursky and Drits, 1984; Tsipursky *et al.*, 1985). Another

interpretation has been based on the analysis of the nearest-neighbor environment of the Fe³⁺ cation by cations having different valences. Goodman (1978) and Eyrish and Dvoretchenskaya (1976a, 1976b) were the first to use this approach; however, they did not support their interpretation of the spectra by electric field gradient (EFG) calculations. Goodman (1976b), who calculated EFG in terms of the point-charge model and later Mineeva (1978) who allowed for orbital overlap contribution, also failed to obtain reasonable results, because the range of probable quadrupole splittings proved to be too narrow to match the experimental half widths. The failure, apparently, was not in the model for the charge distribution in ions, but rather in

the atomic coordinates that were used in these calculations. Obviously, both the size and the shape of a Fe^{3+} -octahedron depend on the charge and the size of the nearest cations. Therefore, the average atomic coordinates provided by diffraction data generally do not correspond to the actual positions of the anions in Fe^{3+} polyhedra having different cationic environments.

A new approach that includes both experimental and simulated structural data was proposed by Daynyak (1980) and Daynyak *et al.* (1984a, 1984b, 1984c), and consists of the following:

1. An analysis of possible combinations of di- and trivalent nearest-neighbor cations to Fe^{3+} based on chemical composition.
2. The simulation of the geometry of the Fe^{3+} -octahedron for each possible combination of the nearest-neighbor cations.
3. A calculation of electric field gradients on Fe^{3+} for different combinations of nearest-neighbor cations in terms of the ionic point-charge model. Apart from being simple, this model allows direct evaluation of the effect of structural distortions on EFG values. Other available calculation methods imply that a change in cation-anion bond lengths leads to significant changes in electron density distribution over atoms, i.e., to a change in effective atomic charges. Such changes require additional parameters to describe the electron density distribution in atoms. Inasmuch as the bonding in 2:1 layer silicates is not purely ionic, it is appropriate to use effective charges instead of ionic charges. If the effective charges are proportional to ionic charges however, with about the same coefficient for all kinds of atoms, calculations may be carried out in terms of the ionic point-charge model. The choice of this model is also justified by the reasonable agreement between experimental O-H vector orientations and those calculated in the point-charge approximation (Bookin *et al.*, 1982).
4. The construction of a model for computer fitting of the Mössbauer spectrum using the EFG calculations and estimates of the expected integrated intensities of the partial components for the mineral involved.

The application of the above approach to the Mössbauer spectra of celadonite, nontronite, "red" muscovite, and glauconite is described below. Special attention is given to the possibilities and limitations of the approximation used.

SIMULATION OF ATOMIC COORDINATES OF AN Fe^{3+} -OCTAHEDRON

At present, none of the experimental methods available allow the true atomic coordinates to be determined for a specific arrangement of di- and trivalent cations in a crystal having cationic substitutions. Thus, the specific structural distortion in a Fe^{3+} -octahedron

can be described only by structure simulation (Baur, 1971; Bookin and Smoliar, 1985). The geometry of a Fe^{3+} -octahedron is uniquely described by individual cation-anion bond lengths, d_i , and bond angles.

To predict d_i , the empirical relation proposed by Baur (1971) was used:

$$d_i = [d_{av} + k(p_i - p_{av})] \text{ \AA}, \quad (1)$$

where d_{av} and k are empirical constants for the given cation-anion pair in the given coordination, p_i is the sum of bond strengths received by the i th anion from the coordinating cations, and p_{av} is the average bond-strength sum for anions in the given polyhedron. The k value for a Fe^{3+} octahedron was estimated by Bookin and Smoliar (1985): $k_{\text{Fe}^{3+}} = 0.4 \pm 0.1$, $d_{av} = 1.98 \text{ \AA}$.

To the first approximation, the octahedral sheet of a 2:1 layer silicate may be considered to have a uniform thickness, h_{oct} , that may be obtained from XRD data. The angle ψ_i between the bond d_i and the normal to the (001) plane is given by

$$\psi_i = \arccos(h_{\text{oct}}/2d_i). \quad (2)$$

Another parameter is the angle $2\chi_i$, which is the angle contained by a pair of individual Fe^{3+} -O,OH bonds, directed to the apices of the "shared" edges. The value for $2\chi_i$ was found using the relevant individual bond length, d_i , and on the mean bond length, d , in the adjacent octahedron:

$$\chi_i = \arccos \left[\frac{3(d_i^2 - d^2 - b^2/9)}{2bd_i} \right], \quad (3)$$

where b is the unit-cell parameter (Drits, 1975). The mean bond length d in a neighboring octahedron corresponds either to R^{3+} or to R^{2+} ; therefore $d_{\text{R}^{3+}} = C_{\text{Fe}^{3+}}d_{\text{Fe}^{3+}} + C_{\text{Al}}d_{\text{Al}}$ and $d_{\text{R}^{2+}} = C_{\text{Fe}^{2+}}d_{\text{Fe}^{2+}} + C_{\text{Mg}}d_{\text{Mg}}$, where C_i is the content of the i th cation and $d_{\text{Fe}^{3+}}$, d_{Al} , $d_{\text{Fe}^{2+}}$, and d_{Mg} are given in Drits (1975). Angles ψ_i and $2\chi_i$ provide a full description of the Fe^{3+} -octahedron geometry for each of its nearest cation environments if d_i and d are known.

EXPERIMENTAL

K-saturated nontronite (from Olhon Island, Lake Baikal), having the composition $\text{K}_{0.44}(\text{Si}_{3.65}\text{Al}_{0.33}\text{Fe}^{3+}_{0.02})(\text{Fe}^{3+}_{1.91}\text{Mg}_{0.09})\text{O}_{10}(\text{OH})_2$, has been preliminarily studied by oblique-texture electron diffraction (Tsipursky *et al.*, 1978). The stacking of 2:1 layers corresponds to polytype 1M, having $a = 5.25$, $b = 9.11$, $c = 10.14 \text{ \AA}$, $\beta = 100^\circ$. The trans-octahedral positions are vacant (Tsipursky and Drits, 1984).

The unit-cell dimensions and composition were included in the crystal-structure simulation procedure (Radoslovich, 1962; Donnay *et al.*, 1964; Bailey, 1966; McCauley and Newnham, 1971; Drits, 1971, 1975; Bookin and Smoliar, 1985). The atomic coordinates

Table 1. Atomic coordinates in the unit cell of nontronite obtained by structure simulation.

Atoms	x/a	y/b	z/c
M	0.0	0.333	0.0
T	0.411	0.314	0.279
K	0.5	0.0	0.5
O ₁	0.351	0.309	0.115
OH	0.424	0.0	0.112
O ₂	0.182	0.254	0.347
O ₃	0.435	0.5	0.322
H ¹	0.256	0.0	0.117

¹ Determined by minimizing electrostatic energy of crystal.

are given in Table 1. The O-H vector orientation was obtained by minimizing the electrostatic energy of the structure.

Celadonite from Zavalye, U.S.S.R (Malkova, 1956), having the composition $(Ca_{0.10}K_{0.89})(Si_{3.96}Al_{0.04})(Al_{0.05}Fe^{3+}_{0.96}Fe^{2+}_{0.26}Mg_{0.73})O_{10}(OH)_2$ is strictly dioctahedral, containing only cis-octahedra occupied as shown by the structural refinement of Drits *et al.* (1984). In accordance with space group *C*2, M2 and M2' cis-positions have different occupancies: $(Mg_{0.65}Fe^{2+}_{0.23}Fe^{3+}_{0.12})$ and $(Mg_{0.12}Al_{0.03}Fe^{3+}_{0.78}Fe^{2+}_{0.05})$, respectively.

The "red" muscovite (Sagn, western Norway) of composition $(Ca_{0.01}Na_{0.05}K_{0.92})(Si_{3.15}Al_{0.85})(Al_{1.48}Ti_{0.04}Fe^{3+}_{0.25}Mn_{0.03}Mg_{0.24})O_{10}(OH)_2$, was treated as an additional example of a model object. The value for the quadrupole splitting Δ was taken from Goodman (1976a). Inasmuch as no structural data exists for this muscovite, the atomic coordinates for 2M₁-muscovite and phengite (Güven, 1971) were averaged in accord with the "red" muscovite's composition.

⁵⁷Fe Mössbauer spectra were recorded at 300 K and 77 K using a LP-4840 spectrometer and a ⁵⁷Co source in a Pd-matrix. The velocity scale was calibrated with reference to α -Fe. The half-width for its spectrum was 0.26 mm/s. To exclude line broadening, the absorbers contained about 5 mg natural Fe/cm². To prepare com-

pletely disoriented samples, the powder was mixed with molten rosin at 360 K, the solidified mixture was further crushed, and the powder was checked by spectra measurements at different tilting of sample support with respect to the direction of the γ -beam. Some problem was noted working with disoriented samples; in contrast to those samples which had not been mixed with molten rosin, their spectra contained a weak Fe³⁺-doublet having $\Delta \sim 1$ mm/s, which is not typical of Fe³⁺ ions in octahedra having predominantly ionic cation-anion bonding. This Δ value appears to be analogous to the anomalous high Δ value (~ 1.3 mm/s) noted for spectra of dehydroxylated layer silicates (Bagin *et al.*, 1980; Daynyak *et al.*, 1981b). In the following discussion the symbol "x" will stand for this doublet.

RESULTS AND DISCUSSION

Possible combinations of di- and trivalent nearest-neighbor cations to Fe³⁺

The most probable combinations of cations in nontronite are [4Si](3Fe³⁺) and [1Al3Si](3Fe³⁺). The combinations [1Al3Si](3Fe³⁺) imply Al occupying one of the two, symmetrically independent tetrahedra (Goodman, 1976b). Inasmuch as vacancies, \square , exist in interlayers, each combination is adjacent to either {2 \square }, {1K₁ \square }, or {2K}. In the following discussion { }, [], and () stand for interlayer, tetrahedral, and octahedral positions, respectively.

In the celadonite under study, tetrahedra and interlayers have homogeneous compositions; thus only octahedral R²⁺ and R³⁺ cations adjacent to the central Fe³⁺ ion must be considered. All such symmetrically independent combinations are presented in Figure 1. As M2 and M2' cis-octahedra in the celadonite studied are not equivalent with respect to the composition of R³⁺ and R²⁺ cations, the number of combinations in Figure 1 is doubled. Thus, along with combinations A, . . . , F for M2 cis-octahedra, the possible presence of Fe³⁺ in M2' octahedra must be considered, together

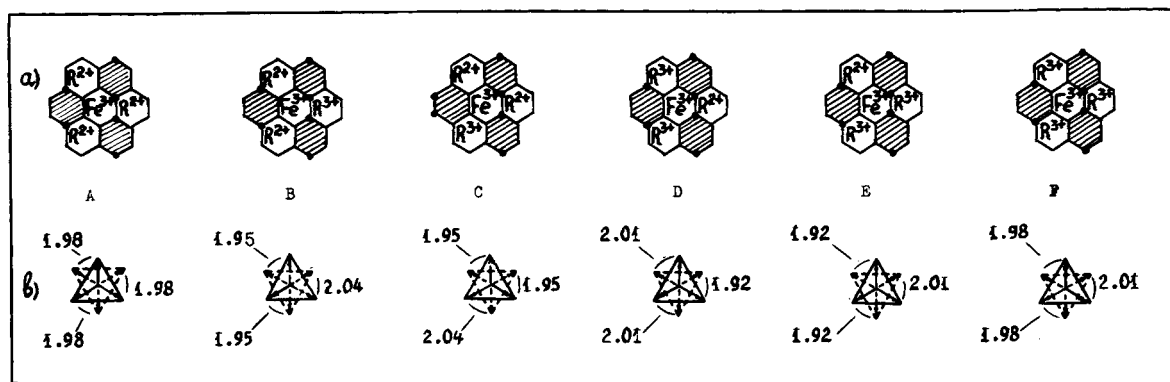


Figure 1. Six possible R²⁺ and R³⁺ cation combinations around Fe³⁺ in M2 cis-positions (a) and the corresponding individual bond lengths d_i in ferric-containing octahedron (b).

Table 2. Angles defining O–H vector orientation in Fe-octahedron,¹ and estimated Δ values for different cation combinations.

Combination	Relative weight for random distribution of cations	ρ_1	ρ_2	ψ_1	ψ_2	$ \Delta $	Δ_{vis} mm/s	Γ_{vis}
				(in degrees ²)				
F1 {2K}[4Si]	0.10	23	23	0	0	0.28	0.33	0.31
	0.29	57	38	0	0	0.32		
	0.21	62	62	0	0	0.35		
F2 {2K}[3Si1Al] = I ³	0.02	33	42	0	-10	0.81	0.82	0.52
	0.02	19	26	2	-37	0.75		
	0.05	62	53	0	-14	0.78		
	0.05	55	29	2	-38	0.85		
	0.04	60	62	-1	-9	0.71		
	0.04	58	60	1	-20	0.70		

¹ Found from the minimum of electrostatic energy.

² ρ = angle between the direction of O–H vector and its projection on plane \vec{ab} (positive direction = to the exterior of octahedral layer), ψ = angle between axis \vec{a} and O–H vector projection on plane \vec{ab} (positive direction = towards the adjacent cis-octahedron; indices "1" and "2" belong to OH-groups of the upper and lower octahedral bases, respectively).

³ Corresponds to positions I and II of Al tetrahedron with respect to Fe³⁺-octahedron (Goodman, 1978).

with corresponding analogous combinations A', B', . . . , F'.

For each possible cation combination, the distortions of the Fe³⁺-octahedron were determined. Individual bond lengths d_i were calculated from Eq. (1) with $k = 0.5$; for celadonite, their values are presented in Figure 1. Angles ψ_i and χ_i were found using formulae (2 and 3).

EFG calculations and analysis of quadrupole splittings

In the present computation program, EFGs were calculated by direct summation over all atoms of the structure, with the exception of the one having $r = 0$ in the area of the radius ≤ 50 Å.

Atomic coordinates for the average unit cell were used over the entire area of summation, except for the anions coordinating the central Fe³⁺. Average charges calculated from the crystal chemical formula were assigned to all cations except those in the central cluster consisting of three octahedral, four tetrahedral, and two interlayer cations nearest to the central Fe³⁺. The distribution of atoms in the cluster was one of the possible particular combinations of di- and trivalent cations.

Table 3. Calculated Δ values for different cation combinations around central Fe³⁺ in celadonite.

Combination	Δ mm/s	$ \Delta _{\text{vis}}$ mm/s
A	0.37	0.36
A'	0.36	
B	0.53	0.52
B'	-0.50	
C	0.52	0.51
C'	0.49	
D	0.43	0.41
D'	0.39	
E	-0.44	0.43
E'	-0.43	
F	0.22	0.17
F'	0.13	

Anion coordinates in the Fe³⁺-octahedron were assigned according to the peculiarities of each given cation combination using Eqs. (2 and 3).

The program for EFG calculation also included minimization of the electrostatic energy for determination of O–H vector orientations. The O–H bond length was assumed to be 0.97 Å (Giese, 1971).

Dealing with model objects has an essential advantage for EFG calculations as the nature of the main component of a spectrum determining the visible splitting is known *a priori*. This fact allowed the EFG calculations to be "fine tuned", i.e., to obtain, by choosing a suitable quadrupole moment, such values for Δ_{calc} that were close to Δ_{vis} . For celadonite the main component is represented by the arrangement (3R²⁺) as shown by the structural refinement (Drits *et al.*, 1984). If the value 0.21 barn (MEDI, 1975) was chosen for the quadrupole moment of the Fe⁵⁷ nucleus, the value of $\Delta_{\text{calc}} = 0.36$ mm/s for the given cation combination was close to the observed splitting of 0.37 mm/s. For nontronite, the splitting is determined, irrespective of the distribution of tetrahedral cations, mainly by [4Si](3R²⁺). The EFG calculations led here also to satisfactory agreement with experiment: $\Delta_{\text{calc}} = 0.33$ mm/s and $\Delta_{\text{vis}} = 0.28$ mm/s. The main component of the muscovite spectrum (Goodman, 1976a) is represented by [4Si](3Al). Here, $\Delta_{\text{vis}} = 0.72$ and $\Delta_{\text{calc}} = 0.74$ mm/s. Such a large Δ value, compared with nontronite, can be explained by the difference in h_{oct} , because the octahedra are occupied by Fe³⁺ in nontronite and by Al in muscovite, implying different Fe³⁺-octahedra flattening (see Eq. (3))—in nontronite, $\psi = 56.1^\circ$, in muscovite, $\psi = 57.1^\circ$.

The results of the EFG calculations for other cation combinations in nontronite and celadonite are given in Tables 2 and 3, respectively. The Δ values in nontronite fall into two groups, namely, F1 and F2. Δ values belonging to group F2 are about 2.5 times greater than those belonging to group F1. Variations in Δ within each group are mainly related to interlayer va-

Table 4. Parameters of Mössbauer spectrum of nontronite ($T_{\text{meas}} = 293 \text{ K}$, $\chi^2 = 1.13$).

Doublet Fe ³⁺	Δ	δ mm/s	Γ	S (%)	S_{F_1}/S_{F_2}
F ₁	0.26	0.39	0.35	57.9	1.81
F ₂	0.64	0.39	0.31	31.4	
tetr.	0.49	0.18	0.29	5.2	
χ^1	1.18	0.42	0.30	5.6	

¹ The doublet resulting from the peculiarities of the preparation of a disoriented sample (see Experimental section).

cancies that affect the O–H vector orientation (Table 2). The Δ values within group F1 are similar to one another, and so are those within group F2. Therefore Δ values within each group have been averaged. Values for the isomer shifts, δ , were assumed to be the same. Thus, from the EFG calculations, the theoretical K-nontronite spectrum should include two doublets corresponding to Fe³⁺ in cis-octahedra, one of which is adjacent to tetrahedral [3Si1R³⁺](F2) and the other to [4Si](F1).

Δ values for each pair of combinations A and A', . . . , F and F' in celadonite were close enough to allow only the corresponding mean values (Table 3) to be considered and to omit the prime. Thus, the theoretical spectrum of celadonite should contain six doublets.

Computer fitting of nontronite and celadonite spectra

The calculated Δ values were used as the initial parameters in the decomposition procedure. Half-widths within a doublet were assumed to be equivalent, the minimum half-width being equal to the apparatus half-width. The ratio of intensities within a doublet was assumed to be unity. Inasmuch as the nontronite spectrum is slightly asymmetric independent of the tilt of the sample support with respect to the γ -beam, the possible presence of Fe³⁺ in tetrahedra was considered. To assign the initial parameters for this doublet, the results of Mössbauer study of tetraferriphlogopite (Pavlishin *et al.*, 1978), and of nontronite were used, where Si is replaced by Fe³⁺ (Goodman *et al.*, 1976). The results for the nontronite spectrum are presented in Table 4 and Figure 2. The experimental ratio $S_{F_1}/S_{F_2} = 1.84$ implies that pairs of Al-tetrahedra with a shared oxygen are forbidden, i.e., Loewenstein's rule is obeyed (Loewenstein, 1954).

To interpret the celadonite spectrum several possible versions had to be analyzed for cation distribution in 2:1 layers. According to the structural data, M2 and M2' cis-octahedra have different R³⁺ and R²⁺ occupancies which decrease considerably the number of possible versions for the distribution of octahedral cations. Because $R^{3+}/R^{2+} = 1$, complete ordering in the celadonite structure implies that the theoretical spectrum should contain only one doublet corresponding

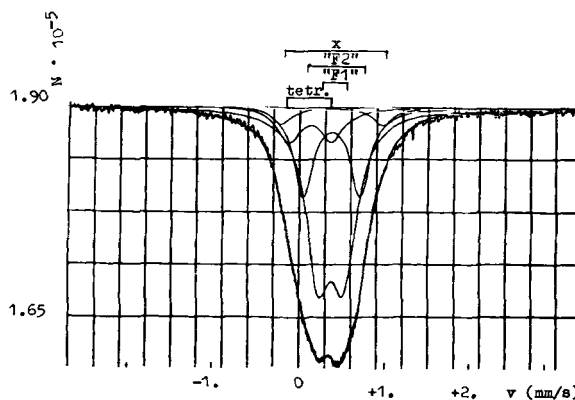


Figure 2. Mössbauer spectrum of nontronite and its computer fitting.

to combination A. Other models may be obtained by adding a set of single exchanges, such as $R^{3+} = R^{2+}$.

Where $R^{3+}/R^{2+} = 1$, complete ordering may be violated due to two types of faults: Fault 1: a pair of cis-octahedra adjacent along b (the shared edge is formed by OH-groups) are occupied by cations of different valence which, as if by mistake, have exchanged their positions (Figure 3a). Fault 2: the pair of adjacent cis-octahedra whose shared edge is formed by OH-groups, are occupied by cations of equal valence. This fault results both from $R^{2+} \rightleftharpoons R^{3+}$ rearrangements in remote cis-octahedra, as shown, for example, in Figure 3b, and from rearrangements in adjacent cis-octahedra whose shared edge is formed by apical oxygens. Table 5 lists relative weights of combinations (A, . . . , F) for the two types of faults, in 10% concentration.¹ About 14% of such isolated faults is a limit, because a larger concentration leads to clusters containing octahedral cations having the same valence. Comparison of the simulated spectra with the experimental one has shown that models with 10% faults are close to the experimental spectrum.

Model predictions (Table 5) have been tested for experimental spectra measured for a random sample with $T_{\text{meas}} = 77$ and $T_{\text{meas}} = 293 \text{ K}$. The computer fitting has shown that model 2, containing faults of type 2, is preferable. Considering the $T = 77 \text{ K}$ spectrum, it is possible, due to the peculiarities in Δ thermal dependence for Fe²⁺ ions, to single out a low-intensity component related to combination F (Figure 4) and to obtain the ratio $A/(B + C + E)$, which is close to that expected for model 2 (Table 6). The presence of this sort of defect, however, is less important than the in-

¹ Ten percent faults of type 1 means that with a fixed direction of the b-axis, the occupancies of 10 pairs of cis-octahedral adjacent to one another along b are $R^{3+}R^{2+}$, and the occupancies of 90 pairs of such octahedra are $R^{2+}R^{3+}$. Ten percent faults of type 2 means that the occupancies of 10 pairs of cis-octahedra are $R^{3+}R^{2+}$, and the occupancies of 90 pairs are $R^{2+}R^{3+}$.

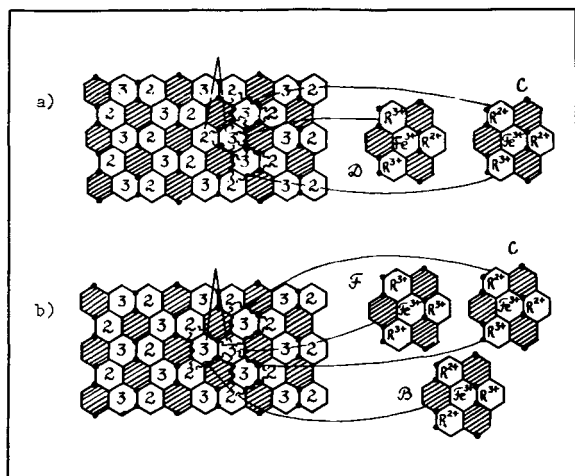


Figure 3. Individual faults, possible in predominantly ordered distribution of cations R^{3+} and R^{2+} in octahedral sheets of celadonite: (a) type 1; (b) type 2.

ference of the high ($\sim 90\%$) degree of cation ordering in the octahedra. This inference does not depend on the type of defects, in agreement with infrared spectroscopic data for celadonite. Relative weights 0.09, 0.21, 0.09, 0.54, 0.03, and 0.04 for bands MgMg, $Fe^{2+}Fe^{3+}$, $Fe^{3+}Fe^{3+}$, Mg Fe^{3+} , $Fe^{2+}Al$, and MgAl in the O–H-stretching region (Figure 5), respectively, found from computer fitting imply only 10% faults for ordered R^{3+} and R^{2+} cation distributions. This concept was discussed in more detail by Slonimskaya *et al.* (1986).

Interpretation of the Mössbauer spectrum of glauconite in terms of the domain model

An interpretation of the glauconite spectrum proposed below should be treated as a first attempt only. This is a specific example which demonstrates the difficulties involved, rather than presents a final solution.

Spectra of glauconite described in the literature may be divided into two groups. Spectra of one type are somewhat better resolved and characterized by a rel-

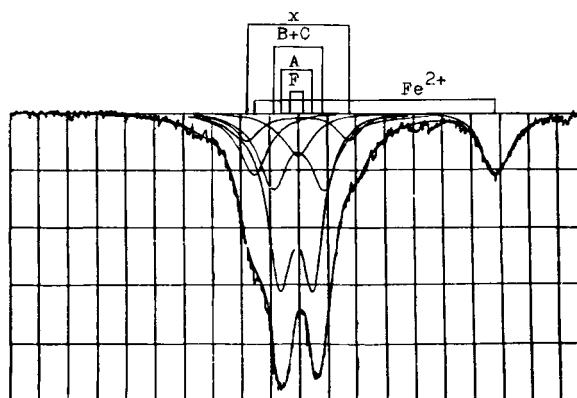


Figure 4. Mössbauer spectrum of celadonite and its computer fitting, $T_{\text{meas}} = 77$ K.

atively smaller total width compared with the spectra of the other type. Relatively wider and more poorly resolved spectra were interpreted conventionally, as described previously (Rozenon and Heller-Kallai, 1978; Govaert *et al.*, 1979; McConchie *et al.*, 1979). The spectra of the first type are approximated by a single doublet with broadened components (Annersten, 1975; Kotlicky *et al.*, 1981), and the corresponding glauconites are considered “ordered”, i.e., having only cis-positions occupied by cations. Interestingly, glauconites of highly heterogeneous composition commonly have better resolved spectra. On the other hand, Slonimskaya *et al.* (1986) showed that the Fe^{3+} –OH–Al band was absent in IR spectra of numerous glauconite specimens. The above considerations suggest that the structures of glauconites that give better resolved Mössbauer spectra consist of muscovite-like and celadonite-like domains, the concentrations of which are determined by the degree of Al-for-Si substitution. These domains may be too small to be revealed by conventional XRD methods.

One of the samples studied here, 68/69-K (Shutov *et al.*, 1972) has a heterogeneous composition ($K_{0.81} Na_{0.01} Mg_{0.01} (Si_{3.78} Al_{0.22})(Al_{0.55} Fe^{3+}_{0.83} Fe^{2+}_{0.24} Mg_{0.40})$)

Table 5. Models for the fitting of Mössbauer spectrum of celadonite.

Doublet Fe^{3+}	Δ mm/s	Γ	The ratio of areas for expected doublets		
			S_A/S_{C+D}	S_A/S_{B+C+E}	S_{B+C+E}/S_F
Model 1: 10% distortions of type 1					
A	0.36	0.27	2.33	—	—
C + D	0.48	0.30			
Model 2: 10% distortions of type 2					
A	0.36	0.27	—	2.17	3.0
B + C + E	0.50	0.30			
F	0.17	0.32			

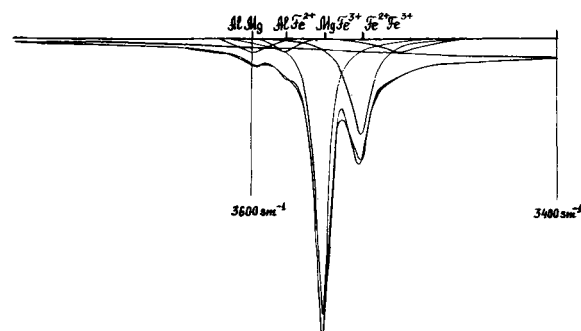


Figure 5. Infrared spectrum of celadonite in the region of the O–H stretching frequencies.

Table 6. Mössbauer spectra parameters for a disoriented sample of celadonite.

Combination and the charge of Fe		Δ	δ (mm/s)	Γ	S (%)	$\frac{S_A}{S_{B+C+E}}$	$\frac{Fe^{3+}}{Fe^{2+}}$	$\frac{S_{B+C+E}}{S_F}$
$T_{meas} = 293 \text{ K}, \chi^2 = 1.15$								
Fe ³⁺	A	0.30	0.37	0.26	51.2	2.6	3.87	—
	B + C + E	0.56	0.37	0.26	19.2			
	x ¹	1.08	0.38	0.26	8.6			
Fe ²⁺		1.09	1.04	0.36	20.5			
$T_{meas} = 77 \text{ K}, \chi^2 = 1.16$								
Fe ³⁺	A	0.32	0.30	0.27	50.2	2.62	3.61	
	B + C + E	0.58	0.30	0.27	19.2			
	x ¹	1.11	0.30	0.27	8.9			
Fe ²⁺		2.55	1.09	0.38	21.7			
$T_{meas} = 77 \text{ K}, \chi^2 = 1.11$								
Fe ³⁺	A	0.37	0.30	0.27	44.1	2.15	3.82	3.01
	B + C + E	0.59	0.30	0.27	20.5			
	F	0.18	0.30	0.27	6.8			
Fe ²⁺	x ¹	1.15	0.31	0.27	9.6			
		2.25	1.07	0.38	19.0			

¹ The doublet resulting from the peculiarities of the preparation of disoriented sample (see Experimental section).

O₁₀(OH)₂) and a relatively well-resolved Mössbauer spectrum. Therefore, its spectrum was initially interpreted in terms of the domain model. According to the above assumption its structure consists of 22% muscovite-like domains (KAl₂Si₃AlO₁₀(OH)₂) and 78% celadonite-like domains (K_{0.8}Al_{0.14}Fe³⁺_{1.06}Fe²⁺_{0.3}Mg_{0.5})Si₄O₁₀(OH)₂). Here, the spectrum was apparently due only to the celadonite-like domains. Even a qualitative consideration of this kind is in a good agreement with the shape of the spectra (Figure 6).

For the celadonite-component of glauconite 68/69-K in which R³⁺ > R²⁺ in octahedra, three doublets should be expected even in the case of complete ordering, namely, a main doublet (3R²⁺) and two low-intensity doublets (3R³⁺) and (2R³⁺, 1R²⁺). Random cation distribution has also been considered. The relative weights for possible cation combinations corresponding to these two extremes are also given in Table 7.

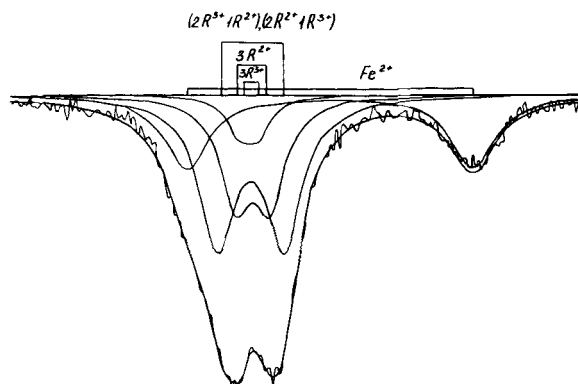


Figure 6. Mössbauer spectrum of glauconite 68/69-K and its computer fitting.

The computer fitting results are given in Table 8 and Figure 6, and the relative weights for corresponding cation combinations are given in Table 7 (last line). Comparison of the two extremes of cation distribution (Table 7) shows that the main indication of ordering is an increase in the relative weight of the (3R²⁺) combination. It is this tendency that is displayed in the computer-fitted glauconite spectrum. The relative weights of the (2R³⁺1R²⁺) and (2R²⁺1R³⁺) combinations are somewhat too high, implying that the real structure tends to deviate from the idealized domain model.

CONCLUSION

From the data discussed above, it is obvious that significant problems arise even for such minerals as nontronite and celadonite in which cation substitutions are mainly in the tetrahedra and octahedra layers, respectively. The reason is in large part due to low resolution of the spectra. As the analysis of such spectra is mathematically incorrect, special modeling is needed. A model for computer fitting should be understood basically as a fixed number of quadrupole doublets and the quadrupole splitting ratio for these doublets. It fol-

Table 7. Relative weights of Fe³⁺ components of the spectrum (percent) corresponding to: I, random cation distribution in domains; II, ideal order of the R³⁺ and R²⁺ over cis-positions in celadonite-like domains; III, computer fitting of the spectrum in terms of the domain model.

	(3R ³⁺)	(3R ²⁺)	(2R ³⁺ 1R ²⁺), (2R ²⁺ 1R ³⁺)
I	22	6	72
II	15	47	38
III	8.9	33.6	57.5

Table 8. Interpretation of Mössbauer spectra of the glauconite 68/69-K sample in terms of the domain model.

Mössbauer parameters	Fe ³⁺			Fe ²⁺
	(3R ³⁺)	(3R ²⁺)	(2R ³⁺ 1R ²⁺), (2R ²⁺ 1R ³⁺)	
Δ (mm/s)	0.17	0.32	0.63	2.73
δ (mm/s)	0.40	0.44	0.42	1.17
Γ (mm/s)	0.27	0.35	0.42	0.52
S (%)	6.5	24.7	42.3	26.5

lows that, apart from the analysis of possible combinations of substituting cations closest to Fe³⁺, EFG can be calculated. EFG calculations require coordinates and charges of ions that take into account their real distribution. Thus, modeling for computer fitting should include several stages each of which involves a certain degree of approximation. In particular, assumptions must be made for the determination of the size and shape of a Fe³⁺-octahedron. For example, uniform thickness h_{oct} is assigned to all octahedra irrespective of the type of adjacent cations. Due to a ± 0.1 error in the k value in Eq. (1) for Fe³⁺, k must be treated as an adjustment parameter used to obtain the Δ range required. Another approximation is the ionic point-charge model used in EFG calculations.

For celadonite and nontronite, the assumptions used for the simulation of a Fe³⁺-octahedron are justified crystalchemically. In general, however, the problem of precise determination of the size and shape of an octahedron that depends on the real distribution of substituting cations is still awaiting solution.

The results of the EFG calculations for the minerals studied imply that the assumption of the constancy of the ratio of effective charges to ionic charges may be reasonable. As mentioned above, substantially different values for the visible splitting are characteristic of the spectra of celadonite, nontronite, and "red" muscovite. The nature of the doublets determining the visible splitting in these spectra was known *a priori*. EFGs were calculated for cation combinations differing both in the sort of cations and the peculiarities of the matrix structure; the same assumptions were used in both cases. The calculations resulted in ratios of the EFG values for the minerals involved that were close to Δ values observed experimentally. Coey *et al.* (1984) reported another example of mineral that can be treated as a model object. In ferripyrophyllite, the value for $\Delta_{\text{vis}} = 0.17$ mm/s results from the combination [4Si(3Fe³⁺)] that corresponds to the combination F in celadonite from Zavalye. This Δ value is exactly the same as Δ_{calc} for the combination F in celadonite (Table 3).

The EFG calculations have shown that some combinations of nearest-neighbor substituting cations to the Fe³⁺ within the same structure lead to similar values of quadrupole splitting. Therefore, a single doublet must be considered that is actually a result of averaging of several doublets. This implies that computer fitting of

the spectrum, if understood as simply a calculation of integrated intensities for the known number of doublets, will not yield information on relative weights of different cation combinations. Thus, a preliminary analysis is necessary for possible versions of cation distribution in the 2:1 layers of mineral, including the determination of theoretical relative weights of cation combinations for each version. A conclusion on the mode of cation distribution may then be drawn by comparing theoretical relative weights of combinations with integrated intensities of partial components produced by the computer fitting of the spectrum.

Preliminary analysis of possible versions of cation distribution for such a mineral as glauconite is a complex task. Because of extensive cationic substitutions in both the octahedral and tetrahedral sheets of glauconite, numerous alternatives may exist. To limit the number of crystalchemically grounded alternatives, other physical methods, in particular IR spectroscopy (Slonimskaya *et al.*, 1986), should be applied. The main efforts for further interpretations of the Mössbauer spectra of glauconite should be directed, first, to the improvement of structural simulation of individual Fe³⁺-octahedra, and, second, to the simulation of crystalchemically justified cation distribution in the 2:1 layers. The interpretation of a Mössbauer spectrum should be preceded by XRD analysis for the occupancies of the cis- and trans-octahedral sites. This analysis is important because trans-octahedra in dioctahedral 2:1 phyllosilicates, i.e., smectites, can be completely or partially occupied (Tsipursky and Drits, 1984). Serious difficulties are also associated with the absence of a refined glauconite structure, due to fine dispersion and structural imperfections. Thus, crystal structure simulation is the only way to obtain precise atomic coordinates, even for the average unit cell. Regression equations used for structure simulation are based on the analysis of numerous reported data on refined phyllosilicate structures and require information only on unit-cell parameters and chemical composition (Smoliar *et al.*, 1984; Bookin and Smoliar, 1985).

In the light of the above requirements for structure simulation, the validity of point-charge approximation for EFG calculations becomes of secondary importance. Clearly, none of the most recent and perfect methods of EFG calculations can give positive results for the cation distribution in glauconite unless the atomic coordinates used in the calculation are reliable.

For the procedure for computer fitting, a similar point of view holds true. Any computer program, no matter how perfect, is bound to fail unless the researcher has worked out a model for computer fitting.

REFERENCES

- Annersten, H. (1975) A Mössbauer characteristic of ordered glauconite: *Neues Jahrb. Mineral. Monatshefte* **8**, 378–384.
 Bagin, V. I., Gendler, T. S., Daynyak, L. G., and Kuz'min,

- R. N. (1980) Mössbauer, thermomagnetic, and X-ray study of cation ordering and high-temperature decomposition in biotite: *Clays & Clay Minerals* **28**, 188–196.
- Bailey, S. W. (1966) Status of clay mineral structures: in *Clays and Clay Minerals, Proc. 14th Natl. Conf., Berkeley, California, 1965*, S. W. Bailey, ed., Pergamon Press, New York, 1–23.
- Baur, W. H. (1971) The prediction of bond length variations in silicon-oxygen bond: *Amer. Mineral.* **56**, 1573–1599.
- Besson, G., Bookin, A. S., Daynyak, L. G., Rautureau, M., Tshipursky, S. I., Tchoubar, C., and Drits, V. A. (1983) Use of diffraction and Mössbauer methods for the structural and crystallochemical characterization of nontronite: *J. Appl. Cryst.* **16**, 374–383.
- Bookin, A. S., Drits, V. A., Rozdestvenskaya, I. V., Semenov, T. F., and Tshipursky, S. I. (1982) Comparison of orientation of OH-bonds in layer silicates by diffraction methods and electrostatic calculations: *Clays & Clay Minerals* **30**, 409–414.
- Bookin, A. S. and Smoliar, B. B. (1985) Prediction of cation-oxygen interatomic distances in coordination polyhedra of the 2:1 layer silicates (pyrophyllite, talc and micas without Li and F): *Mineralogicheskyy Zhurnal* **7**, 51–59 (in Russian).
- Coey, J. M. D., Chukhrov, F. D., and Zvyagin, B. B. (1984) Cation distribution, Mössbauer spectra, and magnetic properties of ferripyrophyllite: *Clays & Clay Minerals* **32**, 198–204.
- Daynyak, L. G. (1980) Interpretation of Mössbauer spectra of some Fe³⁺-containing layer silicates on the basis of structural modelling: Ph.D. thesis, Geological Institute, U.S.S.R., Academy of Sciences, Moscow (in Russian), p. 18.
- Daynyak, L. G., Bookin, A. S., Drits, V. A., and Tshipursky, S. I. (1981a) Mössbauer and electron diffraction study of cation distribution in celadonite: *Acta Crystallogr.* **A37** (suppl.), C-362.
- Daynyak, L. G., Bookin, A. S., and Drits, V. A. (1984a) Interpretation of Mössbauer spectra of dioctahedral Fe³⁺-containing 2:1 layer silicates. II. Nontronite: *Kristallografiya* **29**, 304–311 (in Russian).
- Daynyak, L. G., Bookin, A. S., and Drits, V. A. (1984b) Interpretation of Mössbauer spectra of dioctahedral Fe³⁺-containing 2:1 layer silicates. III. Celadonite: *Kristallografiya* **29**, 312–321 (in Russian).
- Daynyak, L. G., Daynyak, B. A., Bookin, A. S., and Drits, V. A. (1984c) Interpretation of Mössbauer spectra of dioctahedral Fe³⁺-containing 2:1 layer silicates. I. Computation of electric field gradients on the basis of structural modelling: *Kristallografiya* **29**, 94–100 (in Russian).
- Daynyak, L. G., Drits, V. A., Kudryavtsev, D. I., Simanovich, I. M., and Slonimskaya, M. V. (1981b) Crystal chemical specificity of trioctahedral smectites—Products of secondary alteration of oceanic and continental basalts: *Dokl. Akad. Nauk S.S.S.R.* **259**, 1458–1462 (in Russian).
- Donnay, G., Donnay, J. D. H., and Takeda, H. (1964) Trioctahedral one-layer micas. II. Prediction of the structure from composition and cell dimension: *Acta Crystallogr.* **17**, 1374–1381.
- Drits, V. A. (1971) Regularities of crystal chemical structure of trioctahedral micas: in *Epigenesis and its Mineral Indicators*, Nauka, Moscow, 96–110 (in Russian).
- Drits, V. A. (1975) Structural and crystal chemical peculiarities of layer silicates: in *Crystal Chemistry of Minerals and Problems of Geology*, Nauka, Moscow, 35–51 (in Russian).
- Drits, V. A., Tshipursky, S. I., and Plançon, A. (1984) Application of a method for the intensity distribution calculations to the electron diffraction structure analysis: *Izv. Akad. Nauk S.S.S.R. Ser. Fiz.* **49**, 1708–1713 (in Russian).
- Eyrish, M. V. and Dvoretchenskaya, A. A. (1976a) Study of Fe³⁺ ions positions and role in the structure of clay minerals with gamma resonance spectroscopy (change in the condition of Fe³⁺ ions under montmorillonite dehydration and dehydroxylation: *Geochemistry* **4**, 597–606 (in Russian)).
- Eyrish, M. V. and Dvoretchenskaya, A. A. (1976b) Study of Fe³⁺ ions positions and role in the structure of clay minerals with gamma resonance spectroscopy (the relation to mineral crystal chemistry): *Geochemistry* **5**, 748–757 (in Russian).
- Giese, R. F. (1971) Hydroxyl orientation in muscovite as indicated by electrostatic energy calculation: *Science* **172**, 263–264.
- Goodman, B. A. (1976a) The Mössbauer spectrum of a ferrian muscovite and its implications in the assignment of sites in dioctahedral micas: *Mineral. Mag.* **40**, 513–517.
- Goodman, B. A. (1976b) The effect of lattice substitutions on the derivation of quantitative site populations from the Mössbauer spectra of 2:1 layer silicates: *J. Phys. Colloque C6* (Supplement au 12) 819–823.
- Goodman, B. A. (1978) The Mössbauer spectra of nontronite: Consideration of an alternative assignment: *Clays & Clay Minerals* **26**, 176–177.
- Goodman, B. A., Russell, J. D., and Fraser, A. R. (1976) A Mössbauer and IR spectroscopic study of the structure of nontronite: *Clays & Clay Minerals* **24**, 53–59.
- Govaert, A., De Grave, E., and Quartier, H. (1979) Mössbauer analysis of glauconites of different Belgian finding places: *J. Phys. Colloque C2*, 442–444.
- Güven, N. (1971) The crystal structure of 2M₁ phengite and 2M₁ muscovite: *Z. Kristallogr.* **134**, 196–212.
- Heller-Kallai, L. and Rozenson, I. (1981) The use of Mössbauer spectroscopy of iron in clay mineralogy: *Phys. Chem. Minerals* **7**, 223–238.
- Kotlicki, A., Szczyrba, J., and Wiewiora, A. (1981) Mössbauer study of glauconites from Poland: *Clay Miner.* **16**, 221–230.
- Loewenstein, W. (1954) The distribution of aluminum in the tetrahedra of silicates and aluminates: *Amer. Mineral.* **39**, 92–96.
- Malkova, K. M. (1956) On the celadonite of Pobuzhye: in *Collected Papers on Mineralogy* **10**, Lvov Geol. Soc. 305–318 (in Russian).
- Malysheva, T. V., Kazakov, G. A., and Satarova, L. M. (1976) Temperature of sedimentary rocks epigenesis according to Mössbauer spectroscopy: *Geochemistry* **9**, 1291–1299 (in Russian).
- McCauley, J. W. and Newnham, R. E. (1971) Origin and prediction of ditrigonal distortion in micas: *Amer. Mineral.* **56**, 1626–1638.
- McConchie, D. M., Ward, J. B., McCann, V. B., and Lewis, D. W. (1979) Mössbauer investigation of glauconite and its geological significance: *Clays & Clay Minerals* **27**, 339–348.
- MEDI (1975) *Mössbauer effect data index covering the 1975 literature*: J. C. Stevens and V. Stevens, eds. Univ. North Carolina at Asheville, 445 pp.
- Minceva, R. M. (1978) Relationship between Mössbauer spectra and defect structure in biotites from electric gradient calculations: *Phys. Chem. Minerals* **2**, 267–277.
- Pavlishin, V. I., Platonov, A. N., Polshin, E. V., Semenova, T. F., and Starova, G. L. (1978) Micas with iron in quadruple coordination: *Zapisky Vses. Mineral. Obshchestva* **107**, 165–176 (in Russian).
- Radoslovich, E. W. (1962) The cell dimensions and symmetry of layer-lattice silicates. Regression relations: *Amer. Mineral.* **47**, 617–636.
- Rozenson, I. and Heller-Kallai, L. (1978) Mössbauer spectra of glauconites reexamined: *Clays & Clay Minerals* **26**, 173–175.
- Russell, J. D., Goodman, B. A., and Fraser, A. R. (1979)

- Infrared and Mössbauer studies of reduced nontronites: *Clays & Clay Minerals* **27**, 63–71.
- Shutov, V. D., Kats, M. Ya., Drits, V. A., Sokolova, A. L., and Kazakov, G. A. (1972) Crystallochemical heterogeneity of glauconite as depending on the conditions of its formation and postsedimentary changes: in *Proc. Int. Clay Conf., Madrid, 1972*, J. M. Serratos, ed., Div. Ciencias C.S.I.C., Madrid, 269–279.
- Slonimskaya, M. V., Besson, G., Daynyak, L. G., Tchoubar, C., and Drits, V. A. (1986) The interpretation of the IR spectra of celadonites and glauconites in the region of OH stretching frequencies: *Clay Miner.* **21**, 377–388.
- Smoliar, B. B., Daynyak, L. G., Bookin, A. S., and Drits, V. A. (1984) Structural features of dioctahedral mica polytypes and their crystal structure simulation: *Collected Abstr. Int. Conf. Crystal Growth and Characterization of Polytype Structures*, Marseille, France, **1984**, 65–66.
- Tsipursky, S. I. and Drits, V. A. (1984) The distribution of octahedral cations in the 2:1 layers of dioctahedral smectites: *Clay Miner.* **19**, 177–193.
- Tsipursky, S. I., Drits, V. A., and Chekin, S. S. (1978) Study of structural ordering of nontronite by means of oblique electron diffraction: *Izv. Akad. Nauk S.S.S.R., Ser. Geol.* **10**, 105–113 (in Russian).
- Tsipursky, S. I., Drits, V. A., and Plançon, A. (1985) Calculation of the intensities distribution in the oblique texture electron diffraction patterns: *Kristallografiya* **30**, 38–44 (in Russian).

(Received 10 July 1985; accepted 6 January 1987; Ms. 1506)